THE JOURNAL OF PHYSICAL CHEMISTRY Letters

Perspective

pubs.acs.org/JPCL

Interaction of Metals with Suspended Graphene Observed by Transmission Electron Microscopy

Recep Zan,[†,‡] Ursel Bangert,[*,‡] Quentin Ramasse,[§] and Konstantin S. Novoselov[†]

[†]School of Physics and Astronomy and [‡]School of Materials, The University of Manchester, Manchester, M13 9PL, United Kingdom

[§]SuperSTEM Laboratory, STFC Daresbury, Daresbury WA4 4AD, United Kingdom

ABSTRACT: In this Perspective, we present an overview of how different metals interface with suspended graphene, providing a closer look into the metal−graphene interaction by employing high-resolution transmission electron microscopy, especially using high-angle dark field imaging. All studied metals favor sites on the omnipresent hydrocarbon surface contamination rather than on the clean graphene surface and present nonuniform distributions, which never result in continuous films but instead in clusters or nanocrystals, indicating a weak interaction between the metal and graphene. This behavior can be altered to some degree by surface pretreatment (hydrogenation) and high-temperature vacuum annealing. Graphene etching is observed in a scanning transmission electron microscope (STEM) under high vacuum and 60 kV electron beam acceleration voltage conditions for all metals, except for Au. This unusual metal-mediated etching sheds new light on the metal−graphene interaction; it might explain the observed higher frequency of cluster nucleation for certain transition metals and might have implications regarding controlled nanomanipulation, that is, for self-assembly and sculpturing of future graphene-based devices.

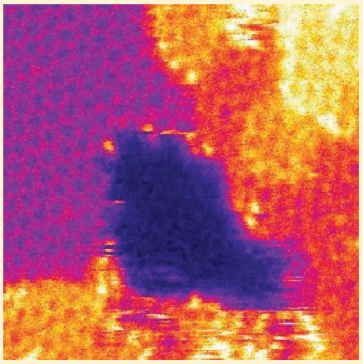

Graphene, the first two-dimensional material to be isolated, has become the focus of intense fundamental research due to its extraordinary properties, but even more so, it has spurred massive interest from various fields into studies regarding nanotechnology applications.[1,2] An area of immense importance in all of this is the study of the metal−graphene interaction because metals have to be used in every single application of graphene as a functional material.[1,3,4] Metal effects on transport, electronic, magnetic, and structural properties of graphene have been investigated both experimentally[3,4] and theoretically[5,6] by means of density functional theory (DFT) with more emphasis on theoretical than on experimental studies.

Due to its large surface area, chemical stability, and low cost, graphene is a highly desirable support for metal catalysts. However, due to the chemical inertness of graphene, there are two barriers to overcome, which affect the metal−graphene interaction, the stabilization of nanoparticles, and achievement of uniform distributions.

Due to its large surface area, chemical stability, and low cost, graphene is a highly desirable support for metal catalysts. However, due to the chemical inertness of graphene, there are two barriers to overcome, which affect the metal−graphene interaction, the stabilization of nanoparticles, and achievement of uniform distributions. Different methods have been suggested to deal with these issues. Introducing vacancies[6,7] and applying strain[8,9] in the graphene sheet are ways of stabilizing metal clusters. Vacancies behave like traps for metal atoms and clusters due to the presence of dangling bonds, thus increasing the reactivity of graphene.[10] The other method consists of functionalizing graphene in solution (graphene oxidation), which also allows one to obtain chemically processable graphene.[11−15] During chemical functionalization, oxy-functional groups are introduced, which act as nucleation sites and facilitate seeding and growth of metal nanoclusters. However, it should be noted that the metal behavior on modified graphene is governed by the chemical method used and can therefore vary.

Graphene has furthermore been used as an ideal transparent support for transmission electron microscopy (TEM) studies directly focused on nanoparticles (i.e., gold[16] and cobalt[17]).

Metals on graphene were found to induce a large enhancement of the Raman signal.[18] A correlation has been recently found between the enhancement factor and the G band splitting for a different number of layers.[19]

Several scanning tunnelling microscopy (STM) studies have been performed to investigate electrical and structural properties of

Received: December 15, 2011
Accepted: March 8, 2012

   dx.doi.org/10.1021/jz201653g | *J. Phys. Chem. Lett.* XXXX, XXX, XXX−XXX

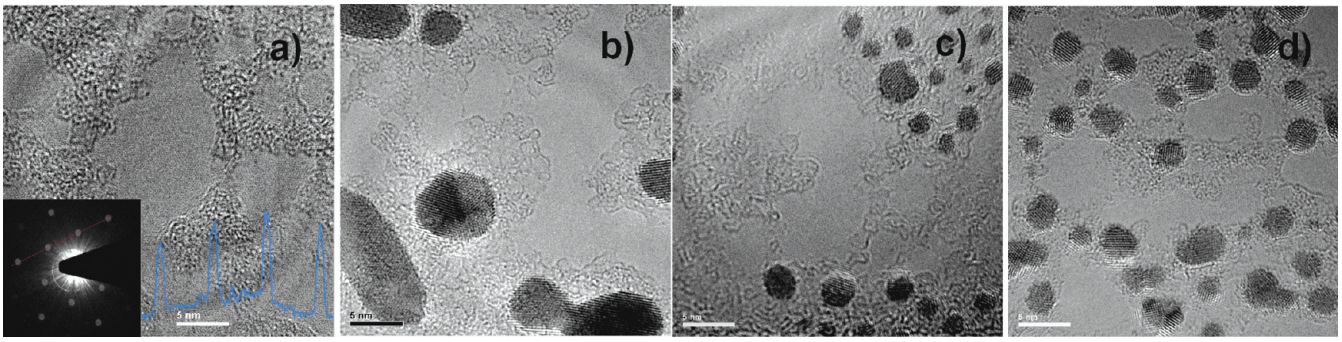

Figure 1. (a) Bright field (BF) image of pristine monolayer graphene. The inset shows the diffraction pattern and intensity profile along the red line in the diffraction pattern. BF image of 2 Å gold evaporated on (b) pristine, (c) two-cycle-hydrogenated, and (d) four-cycle hydrogenated monolayer graphene. The scale (5 nm) is chosen to be same in all images for accurate comparison.

cluster arrays on graphene. However, all reported STM studies are performed on graphene on a substrate; therefore, substrate effects have to be taken into consideration, in particular, when compared to TEM studies, which are conducted on suspended graphene.[20−22]

Metals are also used for graphene tailoring, that is, for cutting graphene sheets into nanoribbons.[23−25] However, the respective experiments are mainly conducted at elevated temperature in gas environments and do not present a controllable way of slicing graphene yet. Metal graphene composites are furthermore used for practical applications, for example, in transistors,[26] electrochemical catalysis,[12] biosensors,[27] solar cells,[28] and batteries.[29]

However, there is a lack of electron microscopy studies, in particular, of high-resolution TEM, and this is limiting the understanding of the metal−graphene interaction. In this Perspective, we present an overview of stationary mode TEM and scanning mode TEM, that is, STEM, of metal−graphene interfaces, providing a closer look into the metal−graphene interaction.

Regardless of the production method, whether produced by exfoliation[1] or CVD growth,[30] suspended pristine graphene is known to react strongly with hydrocarbons. These most probably arise from air exposure and/or remnants of adhesives used during extraction, transfer, and handling of graphene (Figure 1a). Although the microscope column has a relatively high vacuum (~10^{-8} Torr), traces of CO, CO_2, and H_2O can be present inside of the instrument itself. Clean graphene areas (free from residue) vary in size from a few nm^2 to a few hundred nm^2; these areas are surrounded by worm-like hydrocarbon contamination (Figure 1a). Prior to metal deposition (in our case, via evaporation) onto the graphene and consecutive (S)TEM investigations, the number of graphene layers was identified. The most convenient method to do this is via electron diffraction by comparing first- and second-order diffraction spot intensities (inset Figure 1a).[31] To begin with, one of the technologically important metals, Au, has been studied. Gold atoms and clusters are mainly observed on hydrocarbon contamination, as previously reported.[32,33] The cluster sizes vary from about 1 to 5 nm in diameter (Figure 1b), and the clusters are not equally distributed on the graphene surface (Figure 1b). As a result of surface treatment, in our case, by exposing pristine graphene samples to a cold hydrogen plasma[34] for one, two (~30 min), and four cycles (~60 min), the cluster distributions and sizes are affected, although clusters remain on hydrocarbon contamination.[35] Gold cluster distributions become more uniform in hydrogenated samples (Figure 1c and d), and cluster sizes become similar, in particular, after four-cycle hydrogenation. Coalescence of gold clusters is observed for both pristine and hydrogenated samples as a result of long electron beam exposure. However, it is much more pronounced in hydrogenated samples. Coalescence is observed within a few seconds on hydrogenated samples, whereas it takes longer (50 s) in pristine samples.

Gold cluster distributions become more uniform in hydrogenated samples, and cluster sizes become similar.

Another way to study metal clusters on graphene is to anneal them either in a gas environment or in vacuum at elevated temperature. In situ annealing and imaging in the microscope in high vacuum is a feasible way to investigate gold cluster stability at high temperatures. As previously observed by our group, annealing pristine samples at ~700 °C in high vacuum is sufficient to eliminate most of the hydrocarbon contamination from the graphene surface. As can be seen in Figure 2a, as the clean graphene areas increase due to evaporation of hydrocarbon contamination during high-vacuum annealing, the gold clusters, which reside in the hydrocarbons, are forced to move toward each other. However, coalescence has not been observed yet at this temperature (Figure 2a and b). As a next step, the annealing temperature was increased to 950 °C, where gold clusters agglomerated, almost melted, and, as a result, have flattened, and no contamination was observed (Figure 2c). Lastly, for comparison, few-layer graphene with the same amount of gold was annealed at 700 °C in high vacuum (Figure 2d). It was found that gold cluster sizes became bigger, and their distributions were less uniform than on monolayer graphene, resulting in much more open space, free from residue, on the graphene surface.

Gold clusters have been observed to react more strongly with few-layer than with monolayer graphene, either via lattice defects or a very thin interlayer of hydrocarbon contamination. Due to the mismatch between the gold and graphene lattice, rotational Moiré effects can be observed directly in lattice images and also by two rotated sets of diffraction spots in the Fourier transform (FFT) of these images (Figure 3a). Moiré effects have not been observed for boron nitride (BN) with similar amounts of gold evaporation (Figure 3b). As can be seen from the inset in Figure 3b, BN and gold diffraction spots coincide. Au clusters on BN also appear to sit exclusively on hydrocarbon layers. The slightly stronger interaction between

dx.doi.org/10.1021/jz201653g | J. Phys. Chem. Lett. XXXX, XXX, XXX−XXX

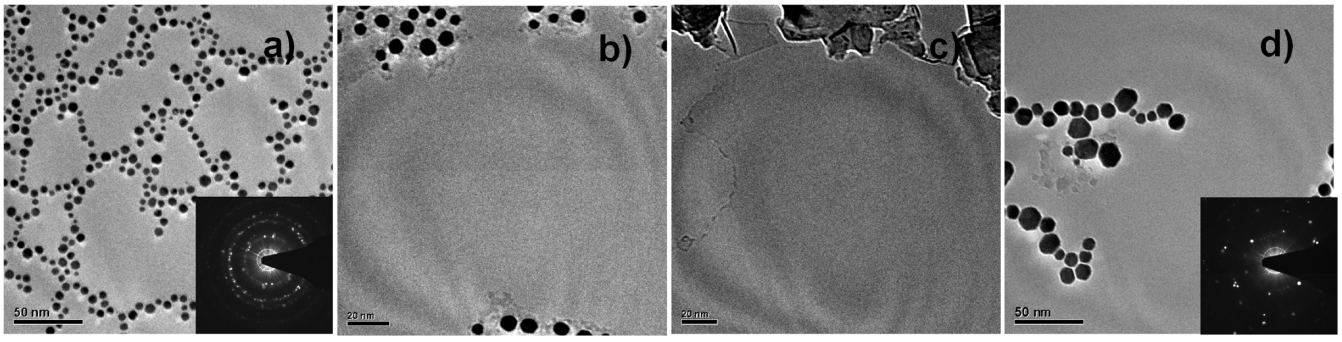

Figure 2. BF images of 2 Å gold (a) evaporated onto monolayer graphene and annealed at 700 °C with the diffraction pattern as the inset, (b) showing a magnified image of (a), (c) as (a) but annealed at 950 °C, and (d) on few-layer graphene and annealed at 700 °C with the diffraction pattern as the inset. The scale bar is the same in (a) and (d), 50 nm, and it is similar in (b) and (c), 20 nm.

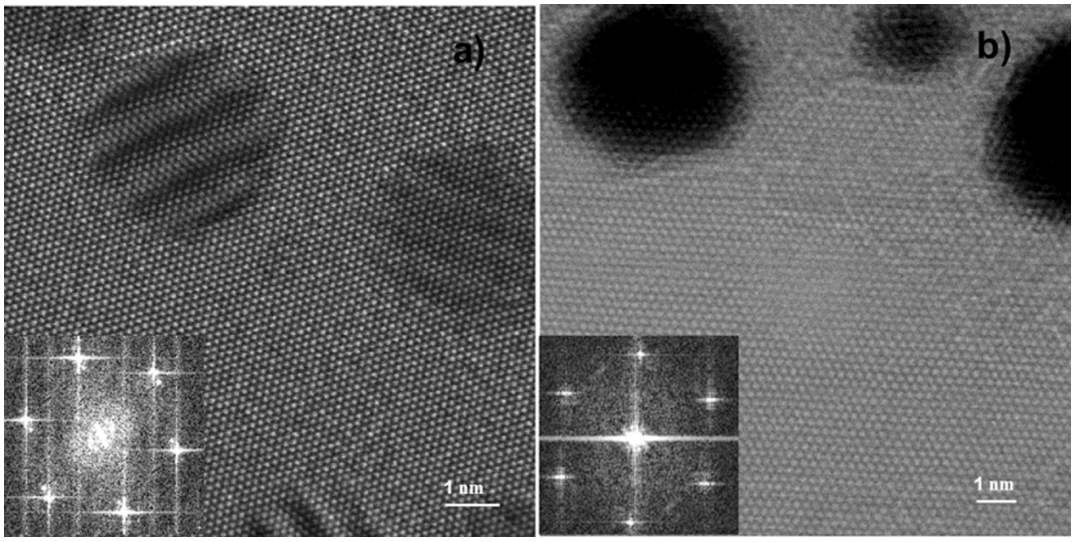

Figure 3. BF images of 2 Å gold evaporated onto few-layer (a) graphene and (b) boron nitride. The corresponding FFTs are shown as insets. The scale bar is the same in (a) and (b), 1 nm.

gold and few-layer graphene in this experiment might be attributed to the higher number (>5) of graphene sheets with subsurface layers making a significant contribution to the bonding, whereas the BN flake was thinner (<5 layers).

Gold has never been observed to introduce any damage into graphene; this conclusion can be drawn with high certainty from STEM studies,[33] where a 60 kV acceleration voltage has been used for imaging, an energy which is known to be well below the displacement threshold for graphene.[36] In contrast, damaging of graphene has been observed in the presence of Al, Ti, Cr, Pd, and Ni, although their interaction with graphene varies; for example, Al, Cr, and Ti are much more reactive than Pd and Ni. Except for a few rare instances, clusters of all of these metals are found to reside on hydrocarbon chains, as for the case of Au. However, observation during repeated STEM scans shows that smaller clusters and individual atoms are drawn out of their initial positions, that is, from the middle of contamination patches to the edge of the contamination. As soon as metals reach the border between the hydrocarbon and clean graphene, they interact with the clean graphene surface. Initially, point defects (vacancies) are created, and this process repeats itself as long as new metal atoms are supplied to the emerging vacancy clusters from nearby metal clusters. Atomic-resolution high-angle annular dark field (HAADF)-STEM imaging has been employed to study individual adatoms on graphene. The scattering probability here follows an approximate Z^2 law, where Z is the atomic number, which makes single-atom impurity detection (especially of impurities heavier than carbon) possible, and the interpretation of the images is rather straightforward.

Damaging of graphene has been observed in the presence of Al, Ti, Cr, Pd, and Ni, although their interaction with graphene varies.

The etching process is shown for Al in the HAADF images in Figure 4. Figure 4a shows a clean, intact graphene patch (black) surrounded by hydrocarbons (gray) with Al clusters (white). Various stages of hole formation are shown in Figure 4b–d, and Figure 4e shows the hole after etching has more or less ceased. In Figure 4b–d, the hole is decorated by newly arriving Al atoms, leading to enlargement, whereas no such atoms can be

dx.doi.org/10.1021/jz201653g | J. Phys. Chem. Lett. XXXX, XXX, XXX–XXX

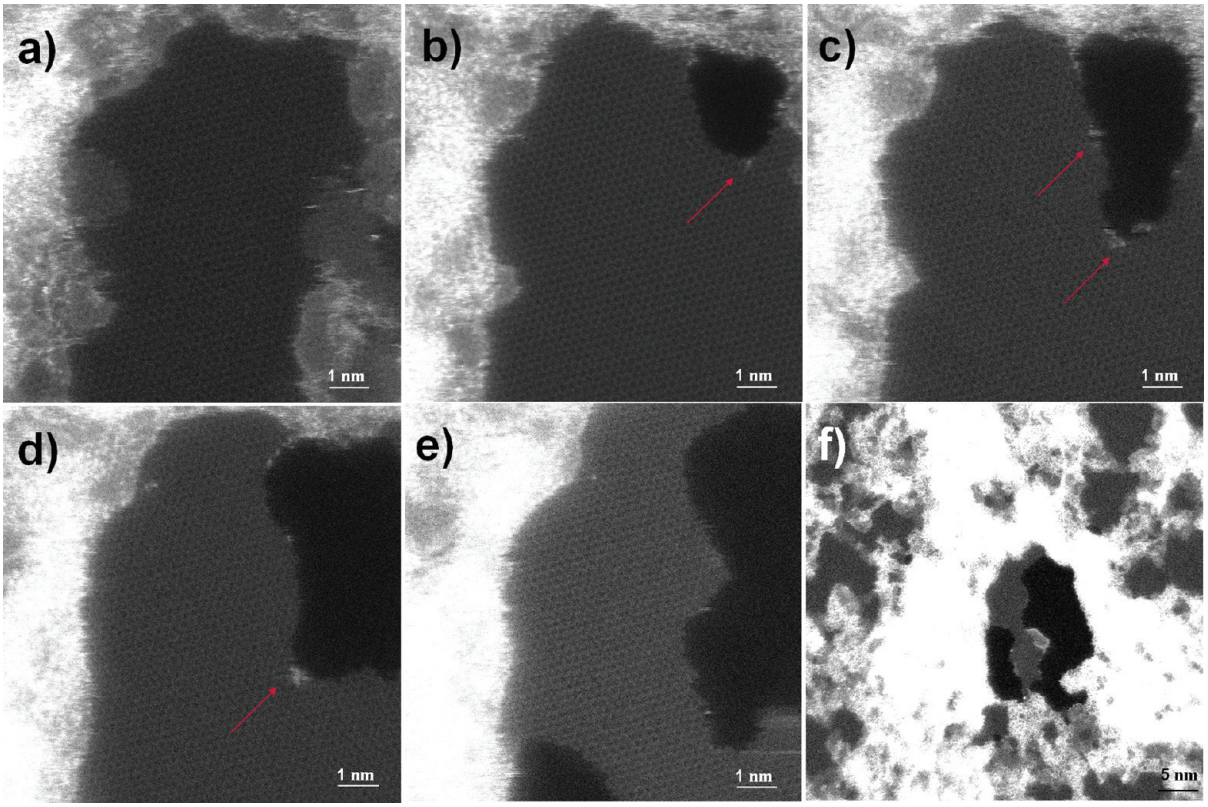

Figure 4. HAADF images of graphene etching in the presence of an aluminum layer of 2 Å nominal thickness (a) before etching, (b) after the start of the hole formation, (c) after hole enlargement in subsequent scans, (d) after continued etching as a result of a sustained supply of Al atoms to the hole's edge (some Al atoms are indicated by red arrows in (b–d), and (e) after the etching process has almost stopped because the Al atom supply has ceased. (f) A lower magnification overview of the Al distribution and hole evolution. The scale bar is the same in (a–e), 1 nm.

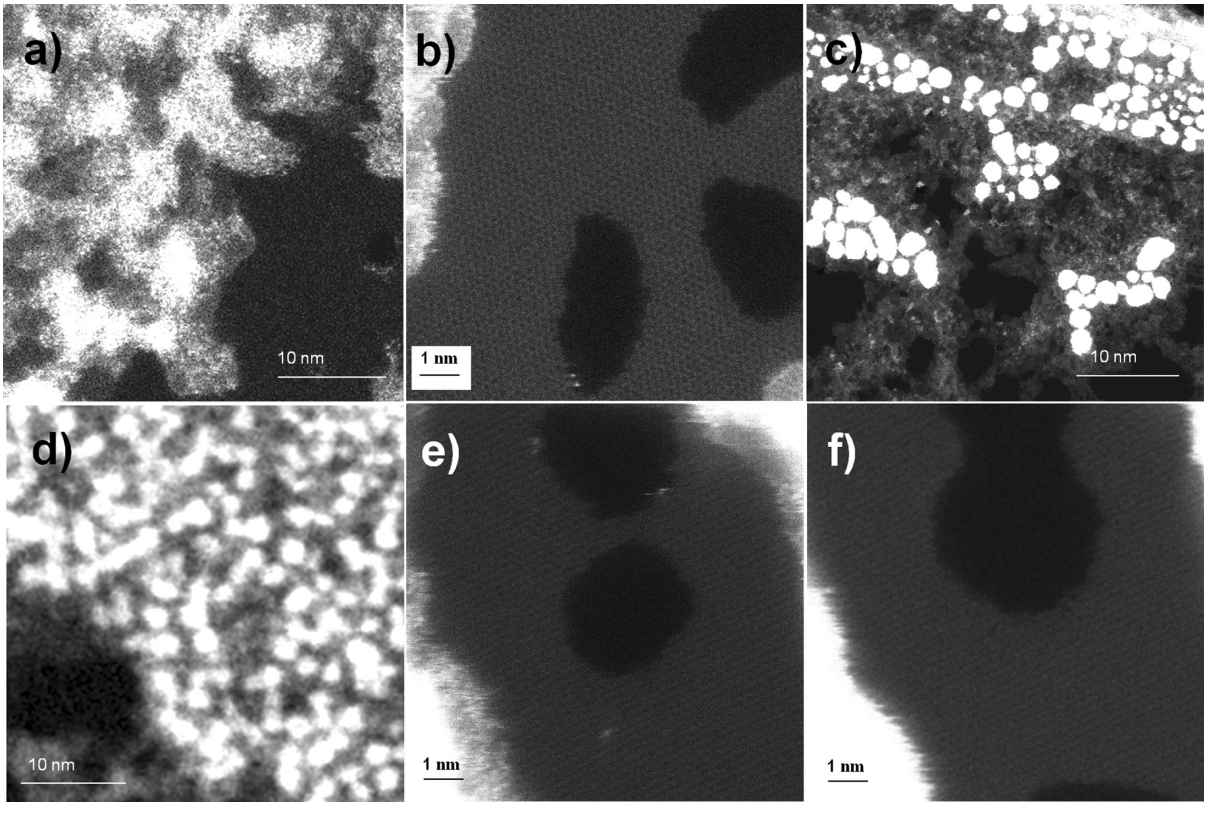

Figure 5. (a) HAADF image (overview) of 2 Å titanium evaporated onto monolayer graphene, (b) a magnified image showing direct etching of the basal plane as a result of the strong interaction between Ti and graphene, (c and d) overview of Pd and Cr distributions on graphene, (e) magnified image showing hole initiation due to Cr at the border of hydrocarbon contamination as well as directly on the basal plane, and (f) coalescence of the holes in (e) after repeated scans.

dx.doi.org/10.1021/jz201653g | J. Phys. Chem. Lett. XXXX, XXX, XXX–XXX

observed in Figure 4e. An overview at smaller magnification of an intermediate etching stage together with the aluminum distribution is shown in Figure 4f. Figure 4 demonstrates clearly that the etching progresses from the border of the contamination into clean graphene as long as metal atoms are present at the hole; these appear to mediate the etching. In the absence of metal atoms at the hole, no such progression of the etching is observed.

This destructive behavior has been predicted by recent DFT calculations of Ni, Al, Co, and Fe on graphene; these elements lower the vacancy formation energy in graphene.[37] The same calculations for Au on graphene do not predict such behavior because vacancy formation energies in this case were found to be similar to those of pristine graphene. However, catalytic oxidation[24] or hydrogenation[26] of carbon atoms in the presence of metal nanoparticles in graphene could be proposed as an alternative mechanism for the etching process. The oxidation mechanisms might be a more valid explanation for our observations as metals are likely to be oxidized during metal evaporation or as a result of exposure to oxygen during handling or in the hydrocarbon contamination. It should be noted that the above cited studies were performed at high temperatures (>650 °C), under gas flow on a substrate, whereas our experiments are performed at room temperature under ultrahigh vacuum conditions. However, although no heat was applied, the energy transferred by the electron beam to the metal−graphene system could be sufficient to activate the etching mechanism, bearing in mind graphene's large heat conductivity; postscanning overviews at lower magnification revealed that holes have also formed in the proximity, that is, outside of consecutively e-beam-scanned areas.

Titanium reacts even more strongly with graphene, as also predicted by DFT calculations,[38] which is reflected in the large binding energy, and thus affects the Ti mobility on graphene. This is confirmed by the appearance of atomic-size aggregates, rather than clusters of Ti on graphene (Figure 5a). Ti has the highest observed dispersion out of the metals studied here. For this reason, Ti atoms do not need to be mobilized over larger distances, and holes form already during the first scan. Although, as in the case of the other metals, Ti is mainly found on hydrocarbon chains, it sometimes resides on clean graphene; this can be witnessed by the fact that etching does not only occur on the border between clean graphene and hydrocarbon deposits but also directly on the basal plane of graphene (Figure 5b). Most recently, because of its thermal stability, palladium has been used in graphene-based devices as an electrical contact[39] and for heterogeneous catalytic applications.[40] Pd has been predicted by recent DFT calculations to form three-dimensional clusters on graphene. This is an indication of its weak interaction with graphene, as also predicted for many other transition metals.[5] We have evidenced that Pd appears in cluster form rather than highly dispersed like Al, Ti, and Cr (Figure 5c). Although the clustering behavior is reminiscent of that of Au on graphene, in contrast to the latter, Pd does etch graphene (not shown).

Chromium is also found to be very reactive with graphene, and, similar to Ti, individual Cr adatoms have been observed on the clean graphene surface. Etching is seen to commence directly in the basal plane as well as at the border between clean graphene and hydrocarbon contamination (Figure 5d). Coalescence of the holes occurs during subsequent scans (Figure 5e).

In summary, we have shown how different metals interact with suspended graphene. All studied metals favor sites on hydrocarbon contamination rather than on the clean graphene surface and present nonuniform distributions, which indicates a weak interaction between the metal and graphene. This behavior is slightly altered with hydrogenation, and it would be worthwhile to investigate other surface treatments, for example, fluorination. High-temperature vacuum annealing is the only way to get rid of the hydrocarbon contamination, which accommodates most of the metal nanoparticles; this is important, for instance, for in situ observations of catalytic activities and of the movement of metal nanoclusters on graphene. Graphene etching is observed for all metals considered in this study, except for Au. This unusual metal-mediated etching of graphene in a STEM in ultrahigh vacuum at 60 kV acceleration voltage sheds new light on the metal−graphene interaction and could be exploited in controlled nanomanipulation and self-assembly processes for future graphene-based devices.

All of the metals studied herein favor sites on hydrocarbon contamination rather than on the clean graphene surface and present nonuniform distributions, which indicates a weak interaction between the metal and graphene.

AUTHOR INFORMATION

Corresponding Author

*E-mail: ursel.bangert@manchester.ac.uk.

Notes

The authors declare no competing financial interest.

Biographies

Recep Zan is currently studying for a Ph.D. in the School of Physics under the supervision of U. Bangert and K. Novoselov at the University of Manchester. He received his B.S. and M.Sc. degrees in Physics from Cukurova University, Turkey. His Ph.D. project is based on transmission electron microscopy of 2D materials, in particular, their interaction with metals.

Ursel Bangert is a Reader in the School of Materials at The University of Manchester. She obtained her Ph.D. from the University of Cologne, Germany. She has contributed to the advancement and exploration of electron microscopies/spectroscopies with ultrahigh spatial resolution. Her research has centred around functional materials and, more recently, nanostructured materials. www.manchester.ac.uk/research/ursel.bangert/

Quentin Ramasse is Scientific Director at the Deresbury SuperSTEM Laboratories, the EPSRC National Facility for Aberration-Corrected STEM. He obtained his Ph.D. from the University of Cambridge and was previously a Staff Scientist at the National Center for Electron Microscopy in Berkeley, California. www.superstem.ac.uk

Konstantin Novoselov is a Professor and Royal Society Research Fellow in the School of Physics at The University of Manchester. He has been awarded the Nobel Prize in Physics, 2010, "for groundbreaking experiments regarding the two-dimensional material

dx.doi.org/10.1021/jz201653g | J. Phys. Chem. Lett. XXXX, XXX, XXX−XXX

graphene". He obtained his Ph.D. from the University of Nijmegen, The Netherlands. His research interests are mesoscopic systems and nanostructures. www.Kostya.graphene.org

■ ACKNOWLEDGMENTS

This work is supported by EPSRC (U.K.).

■ REFERENCES

(1) Novoselov, K. S.; Geim, A. K.; Morozov, S. V.; Jiang, D.; Zhang, Y.; Dubonos, S. V.; Grigorieva, I. V.; Firsov, A. A. Electric Field Effect in Atomically Thin Carbon Films. *Science* **2004**, *306*, 666−669.

(2) Geim, A. K.; Novoselov, K. S. The **rise of graphene**. *Nat. Mater.* **2007**, *6*, 183−191.

(3) Pi, K.; McCreary, K. M.; Bao, W.; Han, W.; Chiang, Y. F.; Li, Y.; Tsai, S. W.; Lau, C. N.; Kawakami, R. K. Electronic Doping and Scattering by Transition Metals on Graphene. *Phys. Rev. B* **2009**, *80*, 075406.

(4) Venugopal, A.; Colombo, L.; Vogel, E. M. Contact Resistance in Few and Multilayer Graphene Devices. *Appl. Phys. Lett.* **2010**, *96*, 013512.

(5) Chan, K. T.; Neaton, J. B.; Cohen, M. L. First-Principles Study of Metal Adatom Adsorption on Graphene. *Phys. Rev. B* **2008**, *77*, 235430.

(6) Krasheninnikov, A. V.; Lehtinen, P. O.; Foster, A. S.; Pyykkö, P.; Nieminen, R. M. Embedding Transition-Metal Atoms in Graphene: Structure, Bonding, and Magnetism. *Phys. Rev. Lett.* **2009**, *102*, 126807.

(7) Boukhvalov, D. W.; Katsnelson, M. I. Chemical Functionalization of Graphene with Defects. *Nano Lett.* **2008**, *8*, 4373−4379.

(8) Cretu, O.; Krasheninnikov, A. V.; Rodriguez-Manzo, J. A.; Sun, L.; Nieminen, R. M.; Banhart, F. Migration and Localization of Metal Atoms on Strained Graphene. *Phys. Rev. Lett.* **2010**, *105*, 196102.

(9) Zhou, M.; Zhang, A.; Dai, Z.; Feng, Y. P.; Zhang, C. Strain-Enhanced Stabilization and Catalytic Activity of Metal Nanoclusters on Graphene. *J. Phys. Chem. C* **2010**, *114*, 16541−16546.

(10) Rodriguez-Manzo, J. A.; Cretu, O.; Banhart, F. Trapping of Metal Atoms in Vacancies of Carbon Nanotubes and Graphene. *ACS Nano* **2010**, *4*, 3422−3428.

(11) Kamat, P. V. Graphene-Based Nanoarchitectures. Anchoring Semiconductor and Metal Nanoparticles on a Two-Dimensional Carbon Support. *J. Phys. Chem. Lett.* **2009**, *1*, 520−527.

(12) Muszynski, R.; Seger, B.; Kamat, P. V. Decorating Graphene Sheets with Gold Nanoparticles. *J. Phys. Chem. C* **2008**, *112*, 5263−5266.

(13) Jasuja, K.; Linn, J.; Melton, S.; Berry, V. Microwave-Reduced Uncapped Metal Nanoparticles on Graphene: Tuning Catalytic, Electrical, and Raman Properties. *J. Phys. Chem. Lett.* **2010**, *1*, 1853−1860.

(14) Pandey, P. A.; Bell, G. R.; Rourke, J. P.; Sanchez, A. M.; Elkin, M. D.; Hickey, B. J.; Wilson, N. R. Physical Vapor Deposition of Metal Nanoparticles on Chemically Modified Graphene: Observations on Metal−Graphene Interactions. *Small* **2011**, *7*, 3202−3210.

(15) Kundu, P.; Nethravathi, C.; Deshpande, P. A.; Rajamathi, M.; Madras, G.; Ravishankar, N. Ultrafast Microwave-Assisted Route to Surfactant-Free Ultrafine Pt Nanoparticles on Graphene: Synergistic Co-reduction Mechanism and High Catalytic Activity. *Chem. Mater.* **2011**, *23*, 2772−2780.

(16) Lee, Z.; Jeon, K.-J.; Dato, A.; Erni, R.; Richardson, T. J.; Frenklach, M.; Radmilovic, V. Direct Imaging of Soft−Hard Interfaces Enabled by Graphene. *Nano Lett.* **2009**, *9*, 3365−3369.

(17) Warner, J. H.; Rummeli, M. H.; Bachmatiuk, A.; Wilson, M.; Buchner, B. Examining Co-Based Nanocrystals on Graphene Using Low-Voltage Aberration-Corrected Transmission Electron Microscopy. *ACS Nano* **2009**, *4*, 470−476.

(18) Schedin, F.; Lidorikis, E.; Lombardo, A.; Kravets, V. G.; Geim, A. K.; Grigorenko, A. N.; Novoselov, K. S.; Ferrari, A. C. Surface-Enhanced Raman Spectroscopy of Graphene. *ACS Nano* **2010**, *4*, 5617−5626.

(19) Lee, J.; Novoselov, K. S.; Shin, H. S. Interaction between Metal and Graphene: Dependence on the Layer Number of Graphene. *ACS Nano* **2011**, *5*, 608−612.

(20) N'Diaye, A. T.; Bleikamp, S.; Feibelman, P. J.; Michely, T. Two-Dimensional Ir Cluster Lattice on a Graphene Moiré on Ir(111). *Phys. Rev. Lett.* **2006**, *97*, 215501.

(21) Sicot, M.; Bouvron, S.; Zander, O.; Rudiger, U.; Dedkov, Y. S.; Fonin, M. Nucleation and Growth of Nickel Nanoclusters on Graphene Moire on Rh(111). *Appl. Phys. Lett.* **2010**, *96*, 093115−3.

(22) Zhou, Z.; Gao, F.; Goodman, D. W. Deposition of Metal Clusters on Single-Layer Graphene/Ru(0001): Factors That Govern Cluster Growth. *Surf. Sci.* **2010**, *604*, L31−L38.

(23) Biró, L. P.; Lambin, P. Nanopatterning of Graphene with Crystallographic Orientation Control. *Carbon* **2010**, *48*, 2677−2689.

(24) Campos, L. C.; Manfrinato, V. R.; Sanchez-Yamagishi, J. D.; Kong, J.; Jarillo-Herrero, P. Anisotropic Etching and Nanoribbon Formation in Single-Layer Graphene. *Nano Lett.* **2009**, *9*, 2600−2604.

(25) Severin, N.; Kirstein, S.; Sokolov, I. M.; Rabe, J. P. Rapid Trench Channeling of Graphenes with Catalytic Silver Nanoparticles. *Nano Lett.* **2008**, *9*, 457−461.

(26) Ponomarenko, L. A.; Geim, A. K.; Zhukov, A. A.; Jalil, R.; Morozov, S. V.; Novoselov, K. S.; Grigorieva, I. V.; Hill, E. H.; Cheianov, V. V.; Falko, V. I.; et al. Tunable Metal−Insulator Transition in Double-Layer Graphene Heterostructures. *Nat. Phys.* **2011**, *7*, 958−961.

(27) Hong, W.; Bai, H.; Xu, Y.; Yao, Z.; Gu, Z.; Shi, G. Preparation of Gold Nanoparticle/Graphene Composites with Controlled Weight Contents and Their Application in Biosensors. *J. Phys. Chem. C* **2010**, *114*, 1822−1826.

(28) Seger, B.; Kamat, P. V. Electrocatalytically Active Graphene−Platinum Nanocomposites. Role of 2-D Carbon Support in PEM Fuel Cells. *J. Phys. Chem. C* **2009**, *113*, 7990−7995.

(29) Chen, D.; Ji, G.; Ma, Y.; Lee, J. Y.; Lu, J. Graphene-Encapsulated Hollow Fe_3O_4 Nanoparticle Aggregates As a High-Performance Anode Material for Lithium Ion Batteries. *ACS Appl. Mater. Interfaces* **2011**, *3*, 3078−3083.

(30) Li, X.; Cai, W.; An, J.; Kim, S.; Nah, J.; Yang, D.; Piner, R.; Velamakanni, A.; Jung, I.; Tutuc, E.; et al. Large-Area Synthesis of High-Quality and Uniform Graphene Films on Copper Foils. *Science* **2009**, *324*, 1312−1314.

(31) Meyer, J. C.; Geim, A. K.; Katsnelson, M. I.; Novoselov, K. S.; Obergfell, D.; Roth, S.; Girit, C.; Zettl, A. On the Roughness of Single- and Bi-layer Graphene Membranes. *Solid State Commun.* **2007**, *143*, 101−109.

(32) Gan, Y.; Sun, L.; Banhart, F. One- and Two-Dimensional Diffusion of Metal Atoms in Graphene. *Small* **2008**, *4*, 587−591.

(33) Zan, R.; Bangert, U.; Ramasse, Q.; Novoselov, K. S. Metal-Graphene Interaction Studied via Atomic Resolution Scanning Transmission Electron Microscopy. *Nano Lett.* **2011**, *11*, 1087−1092.

(34) Elias, D. C.; Nair, R. R.; Mohiuddin, T. M. G.; Morozov, S. V.; Blake, P.; Halsall, M. P.; Ferrari, A. C.; Boukhvalov, D. W.; Katsnelson, M. I.; Geim, A. K.; et al. Control of Graphene's Properties by Reversible Hydrogenation: Evidence for Graphane. *Science* **2009**, *323*, 610−613.

(35) Zan, R.; Bangert, U.; Ramasse, Q.; Novoselov, K. S. Evolution of Gold Nanostructures on Graphene. *Small* **2011**, *7*, 2868−2872.

(36) Egerton, R. F.; Wang, F.; Crozier, P. A. Beam-Induced Damage to Thin Specimens in an Intense Electron Probe. *Microsc. Microanal.* **2006**, *12*, 65−71.

(37) Boukhvalov, D. W.; Katsnelson, M. I. Destruction of Graphene by Metal Adatoms. *Appl. Phys. Lett.* **2009**, *95*, 023109.

(38) Giovannetti, G.; Khomyakov, P. A.; Brocks, G.; Karpan, V. M.; van den Brink, J.; Kelly, P. J. Doping Graphene with Metal Contacts. *Phys. Rev. Lett.* **2008**, *101*, 026803.

(39) Xia, F.; Perebeinos, V.; Lin, Y.-m.; Wu, Y.; Avouris, P. The Origins and Limits of Metal−Graphene Junction Resistance. *Nat Nano* **2011**, *6*, 179−184.

(40) Jin, Z.; Nackashi, D.; Lu, W.; Kittrell, C.; Tour, J. M. Decoration, Migration, and Aggregation of Palladium Nanoparticles on Graphene Sheets. *Chem. Mater.* **2010**, *22*, 5695−5699.